# A novel vectorcardiographic analysis technique to identify ischemic patients

Raúl Correa[a,*], Pedro David Arini[b, c], Máximo Valentinuzzi[c] and Eric Laciar[a]

[a]Gabinete de Tecnología Médica, Facultad de Ingeniería, Universidad Nacional de San Juan (UNSJ), San Juan, Argentina, rcorrea@gateme.unsj.edu.ar; laciar@gateme.unsj.edu.ar

[b]Instituto Argentino de Matemática (IAM) "Alberto P. Calderón", Consejo Nacional de Investigaciones Científicas y Técnicas (CONICET), Buenos Aires, Argentina, pedro.arini@conicet.gov.ar

[c]Instituto de Ingeniería Biomédica (IIBM), Facultad de Ingeniería (FI), Universidad de Buenos Aires (UBA), Buenos Aires, Argentina, maxvalentinuzzi@arnet.com.ar

*Corresponding author:
Raúl Correa
Gabinete de Tecnología Médica - Facultad de Ingeniería
Universidad Nacional de San Juan
Av. Libertador General San Martín 1109 (O)
J5400ARL - San Juan, Argentina
Tel: + 54 - 264 – 4211700 (Ext. 313)
Email Address: rcorrea@gateme.unsj.edu.ar

## Abstract

New signal processing techniques have enabled the use of the Vectorcardiogram (VCG) for the detection of cardiac ischemia. Thus, we studied this signal during ventricular depolarization in 80 ischemic patients, before undergoing angioplasty, and 52 healthy subjects with the objective of evaluating the vectorcardiographic difference between both groups leading to their subsequent classification. For that matter, seven QRS-loop parameters were analyzed, i.e: a) Maximum Vector Magnitude; b) Volume; c) Planar Area; d) Maximum Distance between Centroid and Loop; e) Angle between XY and Optimum Planes; f) Perimeter and, g) Ratio Between Area and Perimeter Loop. For comparison, the conventional ST-Vector Magnitude ($\boldsymbol{ST}_{\mathrm{VM}}$) was also calculated. The results obtained indicate that several vectorcardiographic parameters show significant differences between healthy and ischemic subjects. The identification of ischemic patients via discriminant analysis using $\boldsymbol{ST}_{\mathrm{VM}}$ produced 73.2% sensitivity and 73.9% specificity. In our study, the QRS-loop parameter with the best global performance was the Volume, which achieved 64.5% sensitivity and 74.6% specificity. However, when all QRS-loop parameters and $\boldsymbol{ST}_{\mathrm{VM}}$ were combined, we obtained 88.5% sensitivity and 92.1% specificity. In conclusion, QRS loop parameters can be accepted as a complement to conventional $\boldsymbol{ST}_{\mathrm{VM}}$ analysis in the identification of ischemic patients.

**Keywords**:

QRS-loop, myocardial ischemia, VCG, ST-Vector Magnitude.

## 1-INTRODUCTION

Cardiac ischemia is characterized by an imbalance between myocardial oxygen supply and demand. It is frequently associated with coronary atherosclerosis, which hinders the normal coronary blood flow. It is well-known that insufficient myocardial cell irrigation reflects in the electrocardiogram (ECG) as ST-segment deviation [1] and T-wave alterations [2, 3]. Besides, Pueyo *et al* demonstrated that the upward and downward slopes of QRS complex decreased during artery occlusion [4]. Similarly, Toledo and Wagner proposed an analysis of high-frequency QRS components to identify cardiac ischemia [5]. In all cases, the amplitude and temporal changes of the QRS complex during an ischemic episode are spatially related to the ischemic area. Physiologically, they might be traced back to conduction disturbances in the ischemic segment. In other words, not only the waveform and segment characteristics of cardiac electrical activity are modified during an episode of hypoperfusion but there is need, too, of searching for new parameters to improve ischemic diagnosis.

Besides, the Vectorcardiogram (VCG) has been proposed to evaluate cardiac changes during ischemia or infarction. In an early work, Wolff used the spatial VCG to study initial, early, and terminal “electrical forces” related to ventricular depolarization and concluded that those “forces” can be more accurately described by VCG than ECG [6]. Sederholm *et al* demonstrated that spatial ST-Vector Magnitude ($\boldsymbol{ST}_{\mathrm{VM}}$) and QRS-Vector Difference ($\boldsymbol{QRS}_{\mathrm{VD}}$) behave as complementary measures in the quantification of evolving myocardial injury after acute coronary occlusion and in the determination of sequels to therapeutic interventions [7]. Eriksson used VCG monitoring to identify myocardial reperfusion at an early stage and to give valuable prognostic information in patients with unstable angina and acute myocardial infarction [8]. Kawahito *et al* concluded that monitoring $\boldsymbol{ST}_{\mathrm{VM}}$ along with its $\boldsymbol{QRS}_{\mathrm{VD}}$ may be useful for identifying myocardial ischemia during carotid endarterectomy [9]. In this way, Dellborg *et al* concluded that monitoring of QRS- and ST-Vector combinations may be a highly sensitive method for detecting myocardial ischemia [10]. Recently, Perez *et al* exposed the advantages of the computerized VCG compared to the ECG, particularly by showing better specificity, sensitivity and accuracy as compared with conventional ECG for the diagnosis of several cardiac pathologies [11]. Hence, the need of new VCG analytical methods to extract hidden diagnostic information appears appropriate and timely.

As a consequence**, the aim of this study is to differentiate a group of ischemic subjects from a population of healthy ones by means of the vectorcardiographic analysis of ventricular depolarization**. For that matter, seven QRS-loop parameters were computed and, afterwards, they were contrasted against the conventional $\boldsymbol{ST}_{\mathrm{VM}}$ within a patient classification scheme. Our hypothesis is that the morphological QRS-loop changes due to myocardial ischemia should contribute to, or even perhaps improve, the identification of such patients. A preliminary study produced promising evidence [12].

**2-MATERIALS**

Raw clinical records were extracted from the PTB diagnostic ECG and STAFFIII databases.

The first one contained the ECG records of 52 healthy subjects (39 men, age 42 +/- 14 yrs, and 13 women, age 48 +/- 19 yrs). The ECGs in this collection were obtained by the National Metrology Institute of Germany. Each record includes 15 simultaneously measured signals: the conventional 12 leads (I, II, III, aVR, aVL, aVF, V1-V6) together with the 3 Frank lead ECGs (X, Y, Z). Each signal is digitized at 1000 Hz, with 16 bits of amplitude resolution [13, 14].

The second database consisted of 80 ischemic patients (50 men, age 60 +/- 12 yrs, and 30 women, age 62 +/- 11 yrs), from the Charleston Area Medical Center in West Virginia, before angioplasty (STAFFIII study). Nine standard ECG leads (V1-V6, I, II, III) were digitized at a sampling rate of 1000 Hz and an amplitude resolution of 0.6 μV. A more extensive description of the STAFF III database is found in [15, 16]. Synthesized orthogonal X, Y and Z leads were obtained from the Kors transform [17]. A recent study has demonstrated that Kors synthesis matrix provides a better estimation of Frank leads than Inverse Dower transform in ischemic patients [18].

**3-METHODS**

Figure 1 illustrates a block diagram of the different stages of the analysis. These stages will be explained in the following subsections.

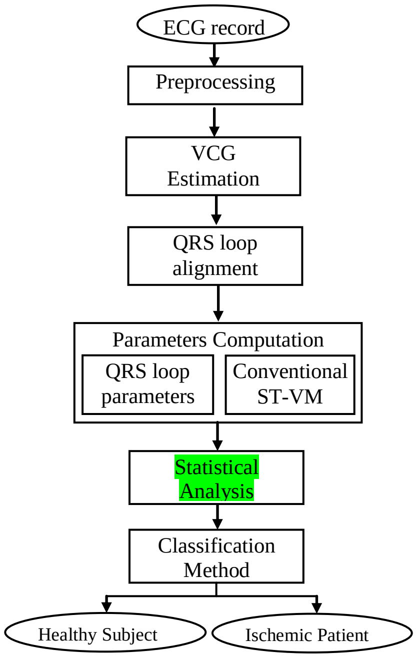


Fig.1. General diagram of the proposed analysis technique.

**2.1-Preprocessing**

Firstly, all ECG records were preprocessed with a band-pass filter (Butterworth, 4$^{th}$ order, 0.2-100 Hz, bidirectional) to reduce low and high frequency noise and a notch filter (Butterworth, 2$^{th}$ order, 50/60 Hz, bidirectional) to minimize the power-line interference. A cubic spline interpolation filter was used to attenuate ECG baseline drifts and respiratory artifacts [19]. Thereafter, the QRS complexes and their endpoints were detected in each ECG record using a modified version of that proposed by Pan and Tompkins [20]. Excessively noisy beats (with a RMS noise level > 40μV, measured in a 40 ms window located at 2/3 of RR interval) were excluded. In addition, ectopic beats were also eliminated by comparing incoming signals against a previously established template with the use of a cross-correlating technique (we used a correlation greater than 95% for acceptance). In this study, a visually low-noise normal beat extracted from the ECG record is selected as a template beat, as it is proposed in [21].

**2.3-VCG Estimation**

The VCG was obtained by drawing simultaneously in a 3-D plot the instantaneous amplitudes of X, Y and Z orthogonal leads for each sample in the temporal interval corresponding to the QRS complex, that is, from the starting point of the Q-wave (or R, if there was no Q) to the final point of the S-wave (or R, if there was no S).

### 2.4-QRS-Loop Alignment

The alignment of all QRS-loops in each ECG record is required in order to compensate the changes induced by extracardiac factors, such as respiratory movements [22]. This alignment can be resolved by obtaining the Rotation (R) and Translation (T) matrices that allow the beat-to-beat QRS-loop alignment against a pattern or template QRS-loop, the latter obtainable from the averaged QRS-complex. In this work we calculated the template QRS-loop as the averaged of each normal sinus QRS-loop, i.e. averaging the temporally aligned QRS complexes in X, Y and Z leads, detected at the first minute of each ECG record using the standard methodology [23].

Such matrices were computed from an adapted version of the algorithm [24], which can be summarized in the following 4 steps:

1) The coordinates X($i$), Y($i$) and Z($i$) of the QRS pattern and QRS individual loop are grouped into, $\{p_i\}$ and $\{q_i\}$ sets, respectively, with $i$ = 1, ..., $N$ and $N$ standing for the total number of samples of the QRS-complex.

2) Both sets $\{p_i\}$ and $\{q_i\}$ are arranged in two 3x$N$ matrices, designed as $P$ and $Q$, respectively; thereafter, the covariance matrix $H$ is determined as $QP^T$.

3) The Singular Value Decomposition technique is applied to the $H$-matrix, wherefrom three matrices result, namely, $U$, $\Lambda$ and $V$, where $H = U\Lambda V^T$; hence, the $R$-matrix can be computed as $R = V\,U^T$.

4) The $T$-matrix is calculated as the difference between the coordinates of the QRS-loop centroid ($p_c$) and the centroid of the individual QRS-loop ($q_c$), that is $T = p_c - R\ x\ q_c$.

Figure 2 illustrates the QRS-loops alignment. On the left side (a), it shows 4 non-aligned QRS-loops with their corresponding centroids and the template QRS-loop, whereas on the right (b), it displays the same 4 QRS-loops after alignment. The small alignment errors observed are produced by normal beat-to-beat morphological differences.

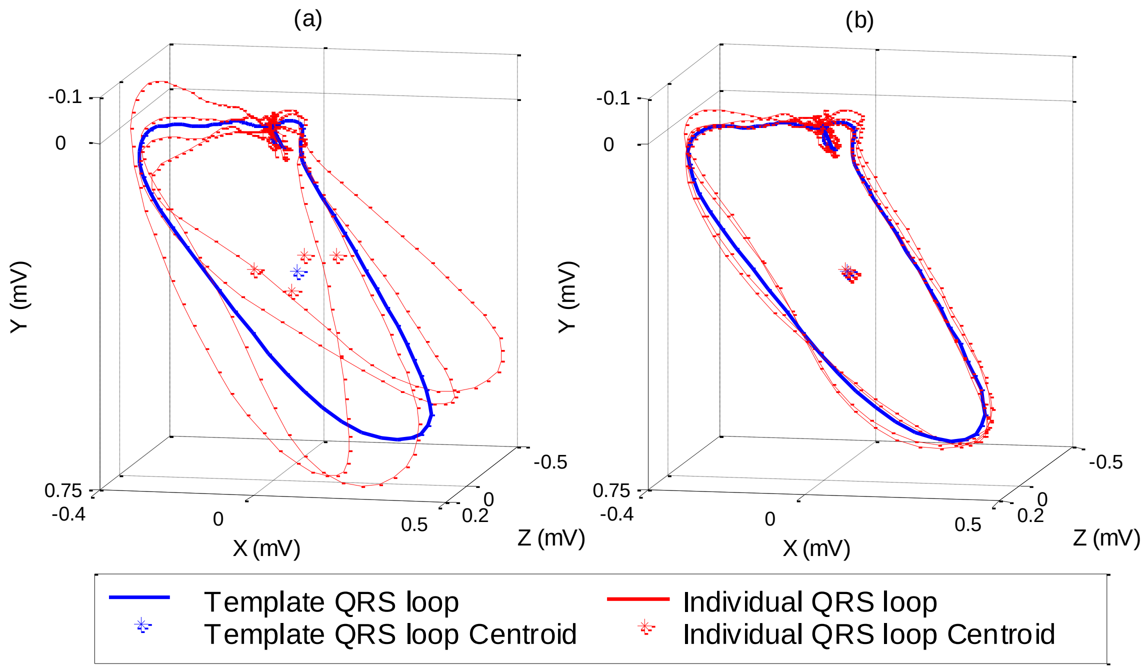


Fig.2. Example of spatial alignment of individual QRS loops for 4 individuals beats extracted from control records of an ischemic patient (Record # 25, STAFFIII Database). (a) QRS loops before alignment. (b) The same QRS loops after alignment.

### 2.5-Parameter Computation

Six vectorcardiographic parameters were computed from the QRS-loop for each detected beat. For comparison, the conventional $\boldsymbol{ST}_{\mathrm{VM}}$ was also computed.

<u>QRS-loop Maximum Vector Magnitude</u> ($\boldsymbol{QRS}_{\mathrm{VM}}^{\mathrm{max}}$): The vector modulus for each QRS coordinate (X, Y, Z) was initially calculated, thereafter, the maximum value was obtained [25]. It describes the maximum magnitude of the Depolarization Vector (Fig. 3).

<u>QRS-loop Volume</u> ($\boldsymbol{QRS}_{\mathrm{V}}$): It estimates the 3-D depolarization loop curve volume and allows quantifying the loop flatness. To achieve a more accurate estimation, it has been found that the point set that produces the minimum convex volume and contains all points within is obtained by means of the Convex Hull algorithm [26].

<u>QRS-loop Planar Area</u> ($\boldsymbol{QRS}_{\mathrm{PA}}$): It is the estimated area of the loop obtained by projecting the QRS-loop on the best adjusted plane computed by least mean squares (denoted as QRS-proj and Optimum Plane, respectively). It is thought to reflect hemodynamic abnormalities in cardiac lesions [27]. The QRS-loop area computed onto optimum plane provides a more exact estimation to the real 3-D QRS-loop area than those calculated on the conventional XY, XZ or ZY planes (Fig. 3).

Maximum Distance between the QRS-centroid and the QRS-loop ($\boldsymbol{QRS}_{\mathrm{DCL}}^{\max}$): The centroid loop is initially estimated and, thereafter, the Euclidean distance from this centroid to each point of the loop is determined searching for its maximum. This parameter measures a relative distance that is independent on the position of the loop in 3-D, unlike $\boldsymbol{QRS}_{\mathrm{VM}}^{\max}$, which measures an absolute distance with respect to the reference system origin (Fig. 3).

Angle between the XY-plane and the Optimum Plane ($\boldsymbol{QRS}_{\mathrm{XYOP}}^{\mathrm{Angle}}$): It evaluates the deviation between the Optimum Plane and the reference frontal plane (XY) in the 3-D space. Since the loops are spatially aligned, the angle variations between both planes are only due to morphological changes of QRS-loop.

Ratio Area/Perimeter ($\boldsymbol{QRS}_{\mathrm{AP}}^{\mathrm{Ratio}}$): This ratio is evaluated over the QRS-loop projected over the Optimum Plane. It served in the analysis of loop morphological changes.

Perimeter ($\boldsymbol{QRS}_{\boldsymbol{P}}$): It is the Perimeter computed over the QRS-loop projected over the Optimum Plane. It measures the loop total length and can detect loop contour changes.

ST-Vector Magnitude ($\boldsymbol{ST}_{\mathrm{VM}}$): It is a widely used parameter in the monitoring of cardiac ischemia [8-9]. It is defined as the magnitude of the vector composed by the X, Y and Z deviations of the ST-segment from the isoelectric level ($\boldsymbol{ST}_{\mathrm{VM}} = \sqrt{ST_X^2 + ST_Y^2 + ST_Z^2}$), measured as the amplitude of the ECG signal at the J-point. This point has been estimated for each beat as $J_k = 40 + 1/3\ (RR_k)^{1/2}$ (in milliseconds), where $k$ denotes the $k$-th beat and $RR_k$ is the RR interval between the this beat and the following one [28].

Figure 3a shows some parameters computed in 3-D plot of an individual QRS-complex extracted from an ECG. Moreover, in Fig. 3b the QRS loop projections on orthogonal conventional planes and the corresponding X, Y, Z ECG leads are shown. The J-point is represented by a red dot.

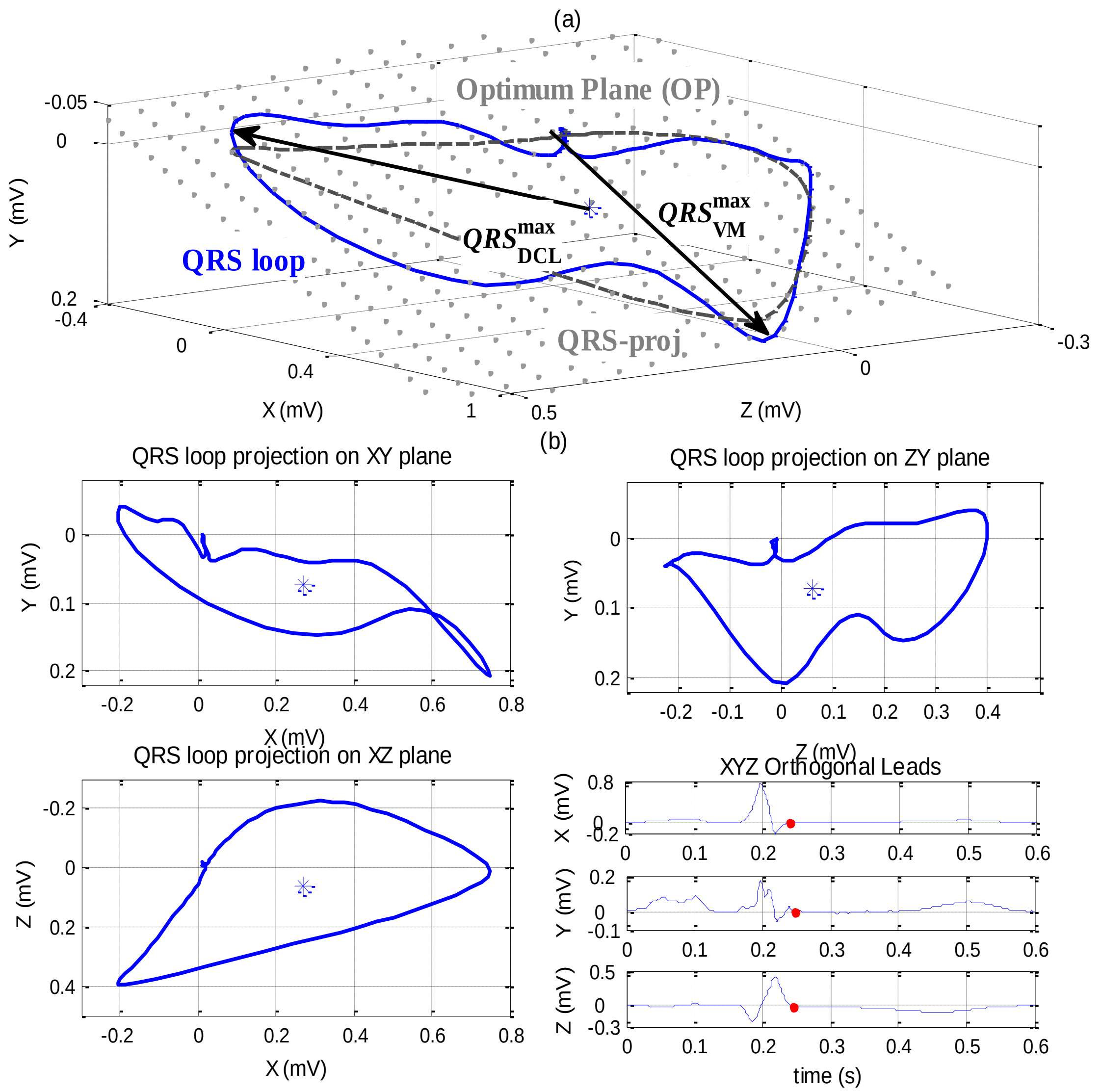


Fig. 3. (a) Some VCG characteristic parameters computed in the 3-D QRS loop for an individual beat extracted from control record of an ischemic patient (Record # 51, STAFFIII Database). (b) QRS loop projections on XY, XZ, YZ planes (frontal, transversal and left sagittal respectively) and temporal representation of X, Y, Z leads with their respective J-point (denoted with a red dot)

### 2.6-Statistical analysis and Classification Method

All described parameters were computed for each detected sinus beat in all ECG records of both populations.

Firstly, we analyzed the normality of this values using D'Agostino-Pearson normality test with the aim to quantify the discrepancy between the distribution parameters value and a Gaussian distribution. Afterwards, comparisons between groups were made using the non-parametric Mann-Whitney tests, because the underlying distribution of the variables was non Gaussian.

Thereafter, the mean value of each parameter across the entire record was calculated. These values were used as inputs to a classifier based on ***Linear Discriminant Analysis (LDA)*** with the aim of distinguishing (or separating out) ischemic patients from healthy subjects.

Basically, a LDA classifier is a linear combination of variables, as follows:

$$y = \mu_0 + \mu_1 X_1 + \mu_2 X_2 + ...... + \mu_p X_p$$

where $y$ is the output value of the discriminant function; $\mu_n$ (with $n=1,..., p$) are the coefficients of the discriminate function; $X_n$ are the discriminate variables (***QRS loop*** parameters and/or ***ST***$_{\mathrm{VM}}$) and $p$ is the number of variables in the analysis [29].

The resulting discriminant function can be used to assign each ECG record to a particular group or class (in this case, ischemic patient or healthy subject), based on its values of discriminate variables. The model coefficients are estimated with a subset of ECG records for which the group is known. This subset of observations is sometimes referred to as the ***training subset*** (we used the 70% of ECG records of both populations).

In order to validate the model, this discriminant function was used to predict the group of another different subset (referred as ***validation subset***) of ECG records (we used the remaining 30% ECG records).

With the aim of evaluate the performance of LDA classifier, we computed the **Receiver Operating Characteristic** (ROC) curve. It is a plot of the Sensibility against the (1-Specificity) values for the different possible cut-off points (we vary the cut-off values between -5 and 5 in 0.01 step) of the discrimination function.

Then, the optimal cut-off point in the ROC curve was computed as the point nearest the top left-hand corner. This selection maximizes the Sensitivity and Specificity sum, when it is assumed that the 'cost' of a false negative result is the same as that of a false positive result [30].

Finally, the global performance of the classifier was evaluated with the Accuracy and the Area Under the ROC Curve (AUC).

## 3-RESULTS

In this study six vectorcardiographic parameters are evaluated on 3-D QRS loop to quantify and assess the morphological differences between ECG recordings of ischemic patients and healthy subjects. Figure 4 illustrates QRS-loops obtained from one regular beat of healthy subject and ischemic patient (the same record illustrated in Fig. 3), respectively. It can be seen that both QRS-loops exhibit important morphologic differences, which we would quantify by the proposed parameters.

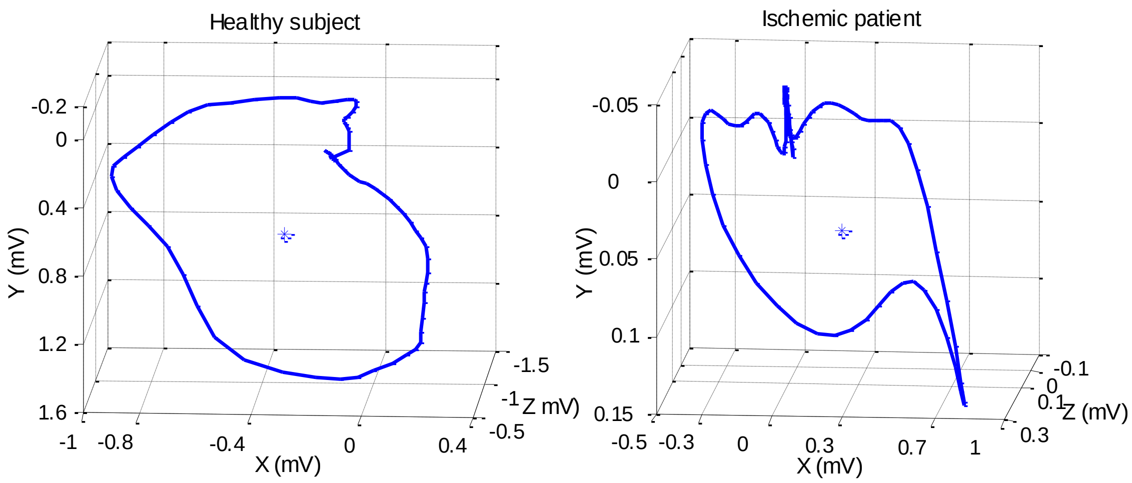


Fig.4. QRS loops of a healthy subject (Record # 2, PTB Database) and an ischemic patient (Record # 51, STAFFIII Database).

Table 1 shows the mean and the standard deviation values computed for each index of both populations. The values marked with * in Table 1 indicate the statistical significance (*p*-value < 0.01).

TABLE 1 MEAN AND THE STANDARD DEVIATIONS OF ***QRS LOOP*** PARAMETERS AND $\boldsymbol{ST}_{\mathrm{VM}}$

| | $\boldsymbol{QRS}^{\max}_{\mathrm{VM}}$ [mV] | $\boldsymbol{QRS}_{\mathrm{V}}$ [mV$^3$] | $\boldsymbol{QRS}_{\mathrm{PA}}$ [mV$^2$] | $\boldsymbol{QRS}^{\max}_{\mathrm{DCL}}$ [mV] | $\boldsymbol{QRS}^{\mathrm{Angle}}_{\mathrm{XYOP}}$ [rad] | $\boldsymbol{QRS}^{\mathrm{Ratio}}_{\mathrm{AP}}$ | $\boldsymbol{QRS}_{\mathrm{P}}$ [mV] | $\boldsymbol{ST}_{\mathrm{VM}}$ [mV] |
|---|---|---|---|---|---|---|---|---|
| Healthy Subjects | 1.55 ± 0.58 | 0.15 ± 0.16 | 1.20 ± 0.65 | 1.03 ± 0.34 | 1.90 ± 0.21 | 4.44 ± 1.92 | 4.84 ± 1.31 | 0.05 ± 0.03 |
| Ischemic Patients | 1.23 ± 0.37* | 0.06 ± 0.06* | 0.79 ± 0.50* | 0.98 ± 0.29 | 1.86 ± 0.22 | 5.45 ± 1.64* | 3.86 ± 0.96* | 0.12 ± 0.10* |

* indicated *p*-value < 0.01, Ischemic patients versus healthy subjects.

Figure 5 illustrates the dispersion of discriminate function values for two different training and validation subsets. The dashed-dot line represent the default cut-off point = 0. It can be observed that the sensitivity and specificity values (computed in the validation stage) are different in (a) respect to (b).

Since these outcomes depends on the records chosen for the training and validation stages (see Fig. 5), we randomly selected 100 different training and validation subsets to obtain more precise results. We used these subsets to computed 100 different discriminant functions.

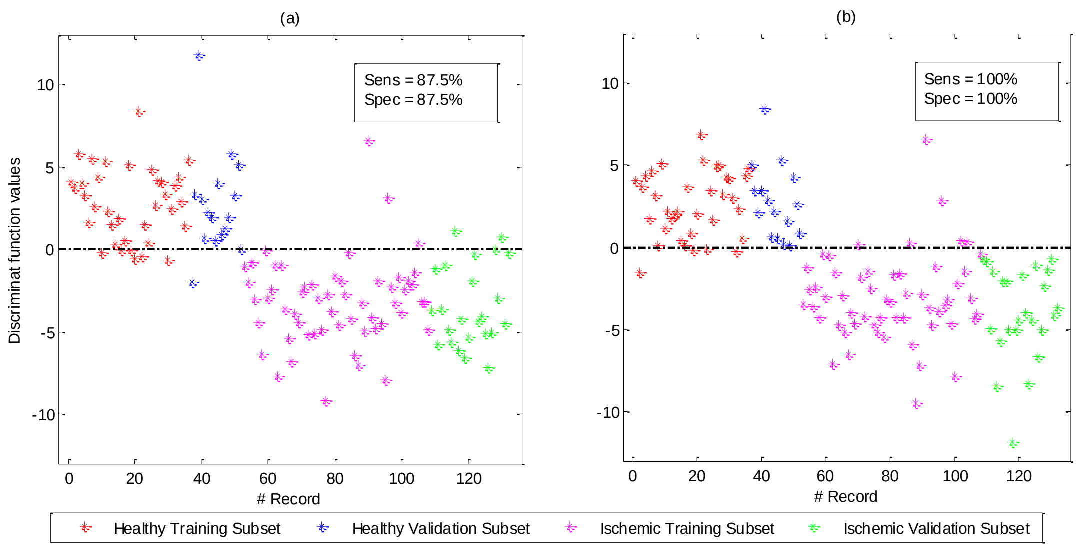


Fig.5. Dispersion of discriminant function values for two different training and validation subsets of healthy and ischemic subjects. The dash-dot line represents the cut-off point (by default equal to 0).

The Fig. 6 shows the ROC curve, built with the mean values of the sensibility and (1-specificity) obtained for the 100 discriminant functions using all QRS-loop parameters and $ST_{VM}$ index. In the same figure we remarked with a red circle the optimum cut-off point and its corresponding Sensibility and Specificity values.

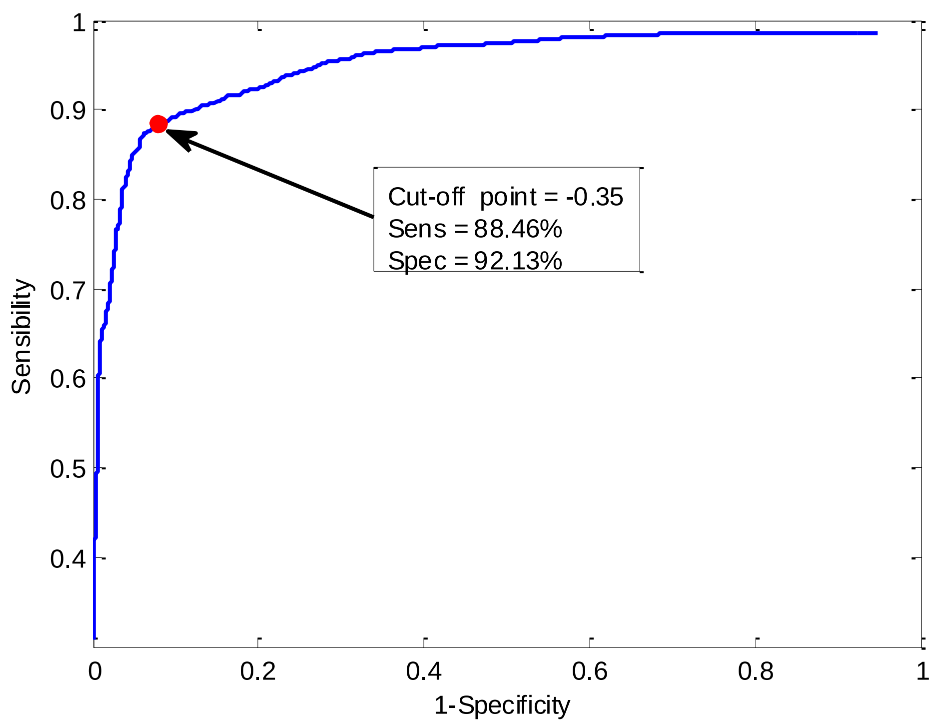


Fig.6. ROC curve and optimum cut-off point has remarked with red circle. For the optimum cut-off point = -0.35 the sensibility is 88.46% and the specificity is 92,13%.

Table II shows the mean values of Sensibility (Sens), Specificity (Spec), optimal cut-off point and the AUC, for different classification schemes using each individual QRS loop parameter, the $\boldsymbol{ST}_{\mathrm{VM}}$ index and the combination of all QRS loop parameters and $\boldsymbol{ST}_{\mathrm{VM}}$.

Table 2. Classification results for ***QRS loop*** parameters and $\boldsymbol{ST}_{\mathrm{VM}}$

| | $\boldsymbol{QRS}_{\mathrm{VM}}^{\max}$ | $\boldsymbol{QRS}_{\mathrm{V}}$ | $\boldsymbol{QRS}_{\mathrm{PA}}$ | $\boldsymbol{QRS}_{\mathrm{DCL}}^{\max}$ | $\boldsymbol{QRS}_{\mathrm{XYOP}}^{\mathrm{Angle}}$ | $\boldsymbol{QRS}_{\mathrm{AP}}^{\mathrm{Ratio}}$ | $\boldsymbol{QRS}_{\mathrm{P}}$ | $\boldsymbol{ST}_{\mathrm{VM}}$ | ***QRS loop*** parameters and $\boldsymbol{ST}_{\mathrm{VM}}$ |
|---|---|---|---|---|---|---|---|---|---|
| Sens (%) | 56.67 | 64.46 | 70.50 | 38.46 | 54.58 | 71.63 | 69.87 | 73.25 | **88.46** |
| Spec (%) | 68.00 | 74.56 | 72.50 | 60.38 | 48.38 | 66.13 | 69.50 | 73.94 | **92.13** |
| Cut-off | -0.66 | -0.72 | -0.61 | -0.49 | -0.43 | -0.50 | -0.33 | -0.27 | **-0.35** |
| AUC | 0.67 | 0.76 | 0.73 | 0.47 | 0.51 | 0.75 | 0.70 | 0.79 | **0.90** |

## 4-DISCUSSION AND CONCLUSIONS

In the last years, numerous papers have proposed different techniques to detect and classify changes in cardiac electrical activity recorded on the surface ECG in patients with myocardial ischemia [1-5]. This cardiopathy is usually diagnosed on the ECG by the measurement of ST deviation at the J-point [31]. However, Pope *et al* showed that only 410 of 1445 patients with acute cardiac ischemia who presented to the emergency departments of ten U.S. hospitals had significant ST deviation [32]. Despite this limitation of the standard electrocardiography, their recordings remain the most important for the clinical evaluation of patients with chest pain [33].

A recent review demonstrates the superiority of the VCG based techniques versus those based on the ECG alone; vectorcardiography provides a better and more rational insight into the electrical phenomena that occurs spatially [11]. Several researchers have proposed the analysis of VCG for studying cardiac diseases, such as myocardial ischemia and infarction [6-10].

The present study examines the 3-D VCG of ischemic patients and healthy subjects to distinguish between them. In order to evaluate the discrepancy in these VCG, six ***QRS loops*** parameters were estimated: $\boldsymbol{QRS}_{\mathrm{VM}}^{\max}$, $\boldsymbol{QRS}_{\mathrm{V}}$, $\boldsymbol{QRS}_{\mathrm{PA}}$, $\boldsymbol{QRS}_{\mathrm{DCL}}^{\max}$, $\boldsymbol{QRS}_{\mathrm{XYOP}}^{\mathrm{Angle}}$, $\boldsymbol{QRS}_{\mathrm{P}}$, and $\boldsymbol{QRS}_{\mathrm{AP}}^{\mathrm{Ratio}}$. For comparison, the conventional $\boldsymbol{ST}_{\mathrm{VM}}$ index was also computed.

On the basis of the descriptive analysis of the studied parameters (shown in Table 1), it can be observed that five QRS-loop parameters and STvm index have significant differences ($p$-value $< 0.01$) between two populations. It indicates that the proposed vectorcardiographic technique can be used to detect the myocardial ischemia.

In addition, the results of the discriminant analysis (shown in Table 2) indicate that $\boldsymbol{QRS}_{\mathrm{V}}$ is the individual QRS-loop parameter with the best global performance (AUC = 0.76), obtaining 64.5% sensitivity and 73.6% specificity. Moreover, the identification of ischemic patients is greatly enhanced when all the QRS-loop parameters in combination with $\boldsymbol{ST}_{\mathrm{VM}}$ index are used in the classification, achieved **88.5% sensitivity and 92.1% specificity.** Meanwhile, when we used only the conventional $\boldsymbol{ST}_{\mathrm{VM}}$ index, we obtained 73.3 % sensitivity and 73.9% specificity, which are considerably lower than those reported above. The poor performance achieved with the ST-level analysis agrees with the study previously reported by Fayne *et al.* [34].

Additionally the AUC values (showed in Table 2) for the classification using all the QRS-loop parameters in combination with $\boldsymbol{ST}_{\mathrm{VM}}$ index is 0.90, which indicates high effectiveness of the proposed classification technique. This AUC value is considered as high accuracy in a diagnostic tests [35].

Furthermore, if we compare the results obtained in this study against those recently reported by A. Dehnavi *et al* [36], it can be concluded that our method has better performance in ischemic patient identification. Ischemia detection technique, based on 22 VCG features and a neural network classifier, obtains 70 % sensitivity and 86% specificity. In contrast, our detection technique achieves 88.5% sensitivity and 92.1% specificity using only 8 VCG parameters and a simple linear classifier.

Briefly, the proposed technique based on QRS-loop study could be used in addition to the traditional $\boldsymbol{ST}_{\mathrm{VM}}$ analysis for a better identification of ischemic patients.

## ACKNOWLEDGMENTS

This study was supported by grants from *Consejo Nacional de Investigaciones Científicas y Técnicas* (PIP 538) and *Universidad Nacional de San Juan*, both institutions from Argentina. The work of Dr. Arini was also supported by a grant from *Fundación Florencio Fiorini*, also from Argentina. The authors would like to thank the anonymous reviewers for their helpful comments.

## REFERENCES

1. Persson E, Pettersson J, Ringborn M, Sörnmo L, Warren SG, Wagner GS, Maynard C, Pahlm O. **Comparison of ST-segment deviation to scintigraphically quantified myocardial ischemia during acute coronary occlusion induced by percutaneous transluminal coronary angioplasty**. *Am. J. Cardiol*. 2006; 97(3):295-300

2. Martínez JP, Olmos S, Wagner GS, Laguna P. **Characterization of repolarization alternans during ischemia: time-course and spatial analysis**. *IEEE Trans. Biomed. Eng.* 2006; 53(4):701-711

3. Arini PD, Baglivo FH, Martínez JP, Laguna P. **Ventricular repolarization dispersion during ischemia course measured by temporal and spatial electrocardiographic parameters**. *Comput. Cardiol*. 2008; 35:323-326

4. Pueyo E, Sörnmo L, Laguna P. **QRS slopes for detection and characterization of myocardial ischemia.** *IEEE Trans. Biomed. Eng*. 2008; 55(2):468-477

5. Toledo E, Wagner GS. **HyperQ-new horizons in ischemia detection**. *J. Electrocardiol*. 2007; 40:S37–S38

6. Wolff L. **The vectorcardiographic diagnosis of myocardial infarction**. *Chest*. 1955; 27:263-281

7. Sederholm M, Grøttum P, Erhardt L, Kjekshus J. **Quantitative assessment of myocardial ischemia and necrosis by continuous vectorcardiography and measurement of creatine kinase release in patients**. *Circulation*. 1983; 68:1006-1012

8. Eriksson S. **Vectorcardiography: a tool for non-invasive detection of reperfusion and reocclusion**. *Thromb. Haemost*. 1999; 82:64-67

9. Kawahito S, Kitahata H, Tanaka K, Nozaki J, Oshita S. **Dynamic QRS-complex and ST-segment monitoring by continuous vectorcardiography during carotid endarterectomy**. *Br. J. Anaesth*. 2003; 90:142-147

10. Dellborg M, Emanuelsson H, Riha M, Swedberg K. **Dynamic QRS-complex and ST-segment monitoring by continuous vectorcardiography during coronary angioplasty**. *Coron. Artery Dis.* 1991; 2(1):43-53

11. Pérez Riera AR, Uchida AH, Ferreira Filho C, Meneghini A, Ferreira C, Schapacknik E, Dubner S, Moffa P. **Significance of vectorcardiogram in the cardiological diagnosis of the 21st century**. *Clin. Cardiol*. 2007; 30:319-323

12. Correa R, Laciar E, Arini PD, Jané R. **Analysis of QRS loop changes in the beat-to-beat vectocardiogram of ischemic patients undergoing PTCA**. *Conf. Proc. IEEE Eng. Med. Biol. Soc.* 2009; 1750-1753

13. Bousseljot R, Kreiseler D, Schnabel A. **Nutzung der EKG-Signaldatenbank CARDIODAT der PTB über das Internet**. *Biomedizinische Technik, Band 40, Ergänzungsband* 1995; 1:S317

14. Kreiseler D, Bousseljot R, **Automatisierte EKG-Auswertung mit Hilfe der EKG-Signaldatenbank CARDIODAT der PTB**. *Biomedizinische Technik, Band 40, Ergänzungsband* 1995; 1:S319

15. García j, Lander P, Sörnmo L, Olmos S, Wagner G, Laguna P. **Comparative study of local and Karhunen-Loeve based ST-T indexes in recordings from human subjects with induced myocardial ischemia**. *Comput. Biomed. Res.* 1998; 31:271–292

16. Pettersson J, Carro E, Edenbrandt L, Pahlm O, Ringborn M, Sörnmo L, Warren GW. **Changes in high frequency QRS components are more sensitive than ST segment deviations for detecting acute coronary artery occlusion**. *J. Amer. College Cardiol*. 2000; 36:1827–1834

17. Kors JA, van Herpen G, Sittig AC, van Bemmel JH. **Reconstruction of the Frank vectorcardiogram from standard electrocardiographic leads: diagnostic comparison of different methods**. *Eur. Heart. J.* 1990; 11:1083-1092

18. Man S, Algra AM, Schreurs CA, Borleffs CJ, Scherptong RW, van Erven L, van der Wall E, Cannegieter SC, Schalij MJ, Swenne CA. **Influence of the vectorcardiogram synthesis matrix on the power of the electrocardiogram-derived spatial QRS-T angle to**

**predict arrhythmias in patients with ischemic heart disease and systolic left ventricular dysfunction**. *J. of Electrocardiol*. 2011; 44:410–415

19. Meyer CR, Keiser HT. **Electrocardiogram baseline noise estimation and removal using cubic spline and state-space computation techniques**. *Comput. Biomed. Res.* 1977; 10:459-470

20. Pan J, Tompkins WJ. **A real-time QRS detection algorithm**. *IEEE Trans. Biomed. Eng.* 1985; 32:230-236

21. Laciar E, Jané R, Brooks DH. **Improved Alignment Method for Noisy High Resolution ECG and Holter Records using Multi-Scale Cross-Correlation**. *IEEE Trans.of Biomed. Eng.* 2003; 50(3):344-353

22. Sörnmo L. **Vectorcardiographic loop alignment and morphologic beat-to-beat variability**. *IEEE Trans. Biomed. Eng.* 1998; 45(12):1401-1413

23. Breithardt G, Cain ME, El-Sherif N, Flowers NC, Hombach V, Janse M, Simson MB, Steinbeck G. **Standards for Analysis of Ventricular Late Potentials using High-Resolution or Signal-Averaged Electrocardiography: A statement by a Task Force Committee of the European Society of Cardiology, the American Heart Association, and the American College of Cardiology**. *Circulation,*1991; 83:1481-1488

24. Arun KS, Huang TS, Blostein SD. **Least-squares fitting of two 3-D point sets**. *IEEE Trans. Pattern. Anal Mach. Intell.* 1987; 9(5):698-700

25. Gannedahls P, Odeberg S, Ljungqvist O, Sollevi A. **Vectorcardiographic changes during laparoscopic cholecystectomy may mimic signs of myocardial ischaemia**. *Acta Anaesthesiol. Scand.* 1997; 41:1187-1192

26. Barber CB, Dobkin DP, Huhdanpaa HT. **The quick hull algorithm for convex hulls**. *ACM Trans. Math. Softw*. 1996; 22(4):469-483

27. Kudaiberdiev Z. **Vectorcardiographic assessment of acute hypoxia effects in pulmonary hypertension due to chronic bronchitis.** *Anadolu. Kardiyol. Derg*. 2007; 7(1):198-200

28. García J, Sörnmo L, Olmos S, Laguna P. **Automatic Detection of ST-T Complex Changes on the ECG Using Filtered RMS Difference Series: Application to Ambulatory Ischemia Monitoring**. *IEEE Trans. Biomed. Eng*. 2000; 47(9):1195-1201

29. Gil Flores J, García Giménez E, Rodríguez Gomez G. **Books of Statistics Nº12: Discriminate Analysis.** *Ed. La Muralla S.A. and Ed. Hespérides S.I.* 2001; 31-57

30. Altman DG. **Practical Statistics for medical Research.** First edition, Published by Chapman & Hall, 2-6 Boundary Row, London SE1 8HN, 1991; 417-418

31. Thygesen K, Alpert J, White H. **Universal Definition of Myocardial Infarction**. *Circulation.* 2007; 116:2634-2653

32. Pope J, Aufderheide T, Ruthazer R, Woolard R, Feldman J, Beshansky J, Griffith J, Selker H. **Missed diagnoses of acute cardiac ischemia in the emergency department**. *N. Engl. J. Med.* 2000; 342:1163–1170

33. Lee T, Goldman L. **Evaluation of the patient with acute chest pain**. *N. Engl. J. Med.* 2000; 342:1187–1195

34. Fayn J, Rubel P, Pahlm O, Wagner G. **Improvement of the detection of myocardial ischemia thanks to information technologies**. *Int. J. of Cardiol*. 2007; 120:172–180

35. Swets JA. **Measuring the accuracy of diagnostic systems**. Science 1988; 240:1.285-1.293

36. Dehnavi A, Farahabadi I, Rabbania H, Farahabadi A, Mahjoob M, Dehnavi N, **Detection and classification of cardiac ischemia using vectorcardiogram signal via neural network**. *J.R.M.S.* 2011; 16(2):136-142

**Figure captions:**

FIGURE 1 General diagram of the proposed analysis technique.

FIGURE 2 Example of spatial alignment of individual QRS loops for 4 individuals beats extracted from control records of an ischemic patient (Record # 25, STAFFIII Database). (a) QRS loops before alignment. (b) The same QRS loops after alignment.

FIGURE 3 (a) Some VCG characteristic parameters computed in the 3-D QRS loop for an individual beat extracted from control record of an ischemic patient (Record # 51, STAFFIII Database). (b) QRS loop projections on XY, XZ, YZ planes (frontal, transversal and left sagittal respectively) and temporal representation of X, Y, Z leads with their respective J-point (denoted with a red dot).

FIGURE 4 QRS loops of a healthy subject (Record # 2, PTB Database) and an ischemic patient (Record # 51, STAFFIII Database).

FIGURE 5 Dispersion of discriminant function values for two different training and validation subsets of healthy and ischemic subjects. The dash-dot line represents the cut-off point (by default equal to 0).

FIGURE 6 ROC curve and optimum cut-off point has remarked with red circle. For the optimum cut-off point = -0.35 the sensibility is 88.46% and the specificity is 92,13%.

**Table Caption:**

TABLE 1. Mean and the standard deviations of ***QRS loop*** parameters and $\boldsymbol{ST}_{\mathrm{VM}}$.

TABLE 2. Classification results for ***QRS loop*** parameters and $\boldsymbol{ST}_{\mathrm{VM}}$